Time-Resolved Studies of CN Radical Reactions and the Role of Complexes in Solution

Andrew C. Crowther, Stacey L. Carrier, Thomas J. Preston, and F. Fleming Crim*

Department of Chemistry, University of Wisconsin − Madison, Madison, Wisconsin 53706

Received: July 21, 2008; Revised Manuscript Received: August 31, 2008

Time-resolved studies using 100 fs laser pulses generate CN radicals photolytically in solution and probe their subsequent reaction with solvent molecules by monitoring both radical loss and product formation. The experiments follow the CN reactants by transient electronic spectroscopy at 400 nm and monitor the HCN products by transient vibrational spectroscopy near 3.07 μm. The observation that CN disappears more slowly than HCN appears shows that the two processes are decoupled kinetically and suggests that the CN radicals rapidly form two different types of complexes that have different reactivities. Electronic structure calculations find two bound complexes between CN and a typical solvent molecule (CH_2Cl_2) that are consistent with this picture. The more weakly bound complex is linear with CN bound to an H atom through the N atom, and the more strongly bound complex has a structure in which the CN bridges Cl and H atoms of the solvent. Fitting the transient absorption data with a kinetic model containing two uncoupled complexes reproduces the data for seven different chlorinated alkane solvents and yields rate constants for the reaction of each type of complex. Depending on the solvent, the linear complex reacts between 2.5 and 12 times faster than the bridging complex and is the primary source of the HCN reaction product. Increasing the Cl atom content of the solvents decreases the reaction rate for both complexes.

I. Introduction

Bimolecular reactions in solution are ubiquitous in chemistry, but there are relatively few studies that explore their mechanisms and dynamics on a time scale comparable to the time between encounters. In addition to the inherent interest of these processes, understanding the properties of thermal bimolecular reactions in solution is a prelude to using vibrational excitation to influence them.[1] Reactions in which CN radicals abstract hydrogen atoms from chlorinated hydrocarbons are particularly attractive candidates for such ultrafast studies, and, indeed, one of the two pioneering studies[2,3] addresses the reaction of CN with chloroform ($CHCl_3$). Photodissociating ICN with 267 nm light generates CN radicals efficiently in solution, and transient absorption using the strong B ← X electronic transition near 388 nm can monitor their evolution.[4] It is also possible to probe the HCN reaction products using transient infrared absorption by the C−H stretching transition near 3.07 μm.[2] Because the C−H stretching transition lies at higher energy in HCN than in alkanes, it is relatively well isolated from interfering transitions in many solvents. The strong C−H bond in the product also makes typical hydrogen abstraction reactions exothermic by about 10 000 cm^{-1},[5] which is enough energy to populate C−H stretching vibrations as high as $v_{CH} = 3$ in the HCN product and makes CN radical reactions suitable for studying product vibrational energy distributions as well.

Detailed studies of gas-phase reactions of CN potentially provide a reference point for comparing reactions in gases and liquids, which can differ substantially because interactions with solvent molecules can change energy barriers and modify the motion along the reaction coordinate. Reactions of CN radicals with most alkanes occur on nearly every gas-phase collision,[6,7] suggesting that there is essentially no barrier to the reaction. The reaction is slower for chloromethanes both in solution and in the gas phase. For example, Samant and Hershberger have measured a rate constant of $(5.4 \pm 0.3) \times 10^8$ $M^{-1}s^{-1}$ for the loss of CN radicals in reaction with $CHCl_3$ in the gas phase,[8] a value that agrees well with the corresponding rate constant of $(4.2 \pm 0.4) \times 10^8$ $M^{-1}s^{-1}$ for the appearance of HCN in solution.[2] However, the populations of the vibrational states of the products show differences that seem to arise from the presence of the solvent. The energy available in gas-phase reactions of CN radicals with hydrocarbons primarily appears as internal excitation of the products,[6,9] in apparent contrast to condensed-phase reactions. The most direct comparison is for the reaction of CN radicals with $CHCl_3$.[6] In the gas phase, it produces an inverted vibrational distribution for the HCN product, with more population in the $v_{CH} = 2$ level than in $v_{CH} = 1$. However, reaction of CN with $CDCl_3$ in solution produces primarily ground-state DCN with only 20% of the products in $v_{CD} = 1$.[2]

Complexes often play an important role in condensed phase reactions. Neta and co-workers have observed complexes of Br in a variety of alkanes and haloalkanes following pulsed radiolysis or laser flash photolysis.[10,11] These complexes are stable for microseconds and can control much of the subsequent chemistry because the reacting entity is a complex rather than a free Br atom.[12] Similarly, Cl radicals form complexes in solution. Chateauneuf has found a strong charge-transfer transition of chlorine complexes with a variety of solvents,[13−15] and Elles et al. have observed a shift of the transient absorption in the first few picoseconds following photolytic production of Cl in CH_2Cl_2 that is consistent with the formation of a Cl complex.[16] There are no comparable studies of CN in solution, but it would be surprising if complexes were not important. Gas-phase studies of CN radical reactions with simple hydrocarbons find negative activation energies that suggest that the reaction proceeds through a weak complex,[7,17−23] and Heaven and co-workers have observed ground electronic state van der Waals complexes of CN with H_2 and Ar in molecular beams.[24−27]

* To whom correspondence should be addressed. E-mail: fcrim@chem.wisc.edu.

10.1021/jp8064079 CCC: $40.75
Published on Web 11/06/2008

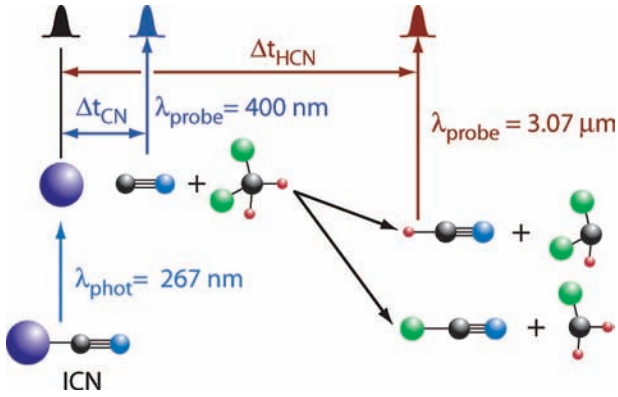

Figure 1. Experimental approach for transient absorption studies of CN reactions. A $\lambda_{phot} = 267$ nm photolysis pulse dissociates the ICN precursor, and probe pulses at either $\lambda_{probe} = 400$ nm or $\lambda_{probe} = 3.07$ μm interrogate the CN reactant or the HCN product respectively, at time delays of Δt_{CN} or Δt_{HCN} following the photolysis pulse. Hydrogen abstraction from CH_2Cl_2 is exothermic by 9700 cm^{-1}, and chlorine abstraction from CH_2Cl_2 is exothermic by 6000 cm^{-1}.

There are also time-resolved studies that use transient absorption to monitor the evolution of photolytically generated CN radicals in $CHCl_3$ solution. Two potential pathways for the abstraction reaction of CN radicals with $CHCl_3$ produce either HCN or ClCN. The hydrogen abstraction channel, producing HCN and CCl_3, is exothermic by 11 300 cm^{-1}, and the chlorine abstraction channel, producing ClCN and $CHCl_2$, is exothermic by 7000 cm^{-1}.[5] Wan et al.[28] and Moskun and Bradforth[29] have followed the isotropic CN radical decay in $CHCl_3$ using the B $\leftarrow$ X electronic transition near 388 nm to observe two distinct timescales. They assign the fast component of a few picoseconds to recombination of the CN radical with I and the slower component of about 70 ps to reaction of the CN radical, results that are consistent with a molecular dynamics simulation of ICN photodissociation in $CHCl_3$.[30] In addition, Moskun et al. have observed the decay of the CN radical anisotropy in several solvents.[29,31]

The goal of the work described here is to use transient absorption to probe the reactions of CN radicals with a range of chlorinated alkane solvents by monitoring *both* the decay of the absorption in the vicinity of the electronic transition of the CN radical and the growth of the infrared absorption of the HCN reaction product. In an earlier study of the reaction of chlorine radicals, we found that the decay rate of the chlorine radical matched the appearance rate of the HCl reaction product, consistent with simple kinetics.[32] The striking result in the study described here is that the decay and appearance rates are *not* commensurate for the reaction of CN with seven different solvents. The transient absorption on the CN radical transition decays between a factor of 2.5 and 12 *more slowly* than the transient absorption of the HCN product grows. Detailed kinetic analysis and electronic structure calculations point to the critical role of rapidly formed complexes that react at different rates.

II. Experimental Approach

The key feature to our approach is generating CN radicals by 267 nm photolysis of ICN with a short pulse of light and probing transient absorption using either the electronic transition of the CN radical reactant or the fundamental C−H stretching transition of the HCN reaction product. Figure 1 illustrates our excitation and detection scheme for the case in which CH_2Cl_2 is the solvent. Following $\lambda_{phot} = 267$ nm photolysis, we probe the CN radical at $\lambda_{probe} = 400$ nm with either a fixed wavelength or a broadband continuum, and we probe the HCN product with infrared light near $\lambda_{probe} = 3.07$ μm. All of the pulses for the experiment come from applying nonlinear optical techniques to a 2.5 mJ, 100 fs pulse of 800 nm light from a Ti:sapphire oscillator and regenerative amplifier operating at 1 kHz. Using this approach, we study CN radical dynamics in seven different solvents (chloroform, dichloromethane, 1,2-dichloroethane, 1,4-dichlorobutane, 2-chloropropane, 2-chlorobutane, and 1-chlorobutane).

A. Photolysis Light. We generate 267 nm photolysis light using two different schemes. For transient UV absorption experiments, a previously described low-power 267 nm arrangement delivers 0.75 μJ pulses to the sample.[33] However, because the HCN infrared transition is about an order of magnitude weaker than the electronic transition of CN, the infrared transient absorption experiments require higher energy photolysis pulses in order for reaction of CN to form enough HCN products. In these experiments, we generate 400 nm light by sending 700 μJ of *p*-polarized 800 nm light through a 3:1 telescope and into a β-barium borate (BBO) crystal (0.3 mm, $\theta = 29°$, type I, *ooe*) and mixing that pulse with 440 μJ of 800 nm light in a second BBO crystal (0.3 mm, $\theta = 42°$, type I, *ooe*), a process that generates 95 μJ of 267 nm light. A grating pair stretches this pulse to 3.25 ps to minimize burning of the sample cell, an arrangement that also minimizes the possibility of multiphoton background signals. The stretcher, which uses 1200 grooves/mm ruled gratings blazed at 250 nm, has an overall efficiency of 25%. In both arrangements, a double Fresnel rhomb rotates the 267 nm pulse to magic-angle polarization (54.7°) with respect to the probe pulse to suppress the effects of anisotropic decay. The energy of the photolysis pulse reaching the sample is 8 μJ.

B. Probe Light. We use three different probe techniques for these experiments. Electronic probing of the CN reactant uses either 400 nm light obtained by doubling 800 nm light from the regenerative amplifier or by generating a broadband continuum. Vibrational probing of the HCN uses 3.07 μm infrared light from a potassium niobate ($KNbO_3$) optical parametric amplifier (OPA). We block half of the photolysis pulses using either a chopper or shutter for active background subtraction, and a computer-controlled translation stage establishes the delay between the photolysis and probe pulses in all of the probe schemes.

The frequency doubling scheme generates 400 nm probe light using a BBO crystal (0.3 mm, $\theta = 29°$, type I, *ooe*). We separate the pulses into a probe beam and a reference beam that we detect with integrating silicon photodiodes, and we average 1000 pulses for each position of the delay stage to achieve a noise level of 50 μOD. At the sample, the diameters of the photolysis and probe beams are 200 and 80 μm full width at half-maximum (fwhm) intensity, respectively. The broadband UV−vis scheme generates a continuum between 350 and 650 nm by focusing a small amount of 800 nm light into a 6 mm thick piece of UV-grade CaF_2. After recollimation and focusing by off-axis parabolic mirrors, both the probe and reference continuum beams enter a modified Czerny−Turner spectrometer. Each beam passes through a polarizer, strikes a 600 grooves/mm grating blazed at 400 nm, and passes through a 50 mm focal length lens before striking separate 512 pixel, 12.5 mm wide silicon photodiode arrays (Hamamatsu, S3904−512Q). We calibrate the arrays using a holmium perchlorate solution (15% w/v) in 10% perchloric acid and use two shutters (Vincent Associates Uniblitz-LS6, Uniblitz-VMM-D4) to obtain the transient signal with and without the photolysis pulse present.

We typically integrate 300 pulses on the photodiodes with and without the photolysis light present and subsequently average 20 to 30 such pairs of data to achieve a noise level of about 1 mOD. At the sample, the diameters of the photolysis and probe beams are 100 and 45 μm (fwhm), respectively.

The continuum-seeded, two-pass OPA that generates infrared light for probing HCN uses a $KNbO_3$ crystal (2 mm, $\theta = 41.5°$, type I). Beginning with 750 μJ of 800 nm light, we generate up to 30 μJ of mid-infrared idler light that we separate into probe and reference beams. The reference beam strikes a single lead−selenide integrating photodiode, and the probe beam passes through the sample and into a 0.25 m monochromator having a 300 grooves/mm grating blazed at 2 μm. The monochromator disperses the probe pulse onto a 32 pixel, 6.7 mm wide mercury cadmium telluride array (Infrared Associates, MCT-10−2 × 32). We calibrate the arrays using 25% by volume solutions of $CHCl_3$ and CH_2Cl_2 in CCl_4. Averaging 10 traces of 5000 pulses for each position of the delay stage produces a noise level of 40 μOD. We focus the photolysis and probe pulses to diameters of 80 and 40 μm fwhm at the sample, respectively.

C. Sample. We use a modified version of the procedures described by Moskun and Bradforth[29] and by Larsen et al.[34] to synthesize ICN. The most important change is an additional recrystallization in cyclohexane.[35] Because purification of the ICN by sublimation does not change the UV−vis spectrum or the time evolution, we use it without further purification. For CN radical detection, we make 0.1 M ICN solutions (OD ≈ 0.9 at 267 nm), and for HCN detection, we make 0.2 M ICN solutions (OD ≈ 1.7 at 267 nm). A Teflon gear pump circulates each 50 mL sample through a 1 mm thick Teflon cell that has 2 mm thick UV-grade MgF_2 windows. We only use a sample for about an hour, when a light-purple color from accumulation of I_2 appears, and find that the observed time evolution at the beginning and end of the sample lifetimes are the same. We use 99.9% CH_2Cl_2 from Mallinckrodt Chemicals. All other solvents come from Sigma-Aldrich: $CHCl_3$, >99.9%; 1,2-dichloroethane, 99.8%; 1,4-dichlorobutane, 99.0%; 2-chloropropane, 99.0%; 2-chlorobutane, 99+%; and 1-chlorobutane, 99.5%.

III. Results

A. Transient Absorption. Photolysis of ICN with 267 nm light creates a transient population of I and CN, and our goal is to probe the evolution of the CN radical and adducts or products that it forms. In general, the radicals can have transitions similar to those of the isolated species but slightly perturbed by the presence of the solvent, and they can also have transitions to excited states in which there is charge transferred between the solvent and the radical. A weakly bound, ground-state complex might have a transition to a charge-transfer state that is strongly bound by the Coulomb interaction between the separated charges. Consequently, these charge-transfer transitions of the complexes can have a substantially lower energy than those of the isolated species. The transition energy increases as the difference in the ionization energy of the electron donor and the electron affinity of the electron acceptor grows, as illustrated by the Cl complexes in which the transition shifts to higher energy as the ionization energy of the solvent increases.[13] These considerations help identify the transition responsible for the transient electronic absorption we observe.

Moskun and Bradforth[29] identify the transition near 380 nm as the B ← X transition of the CN radical, a conclusion that is consistent with the transition we observe in the same region in

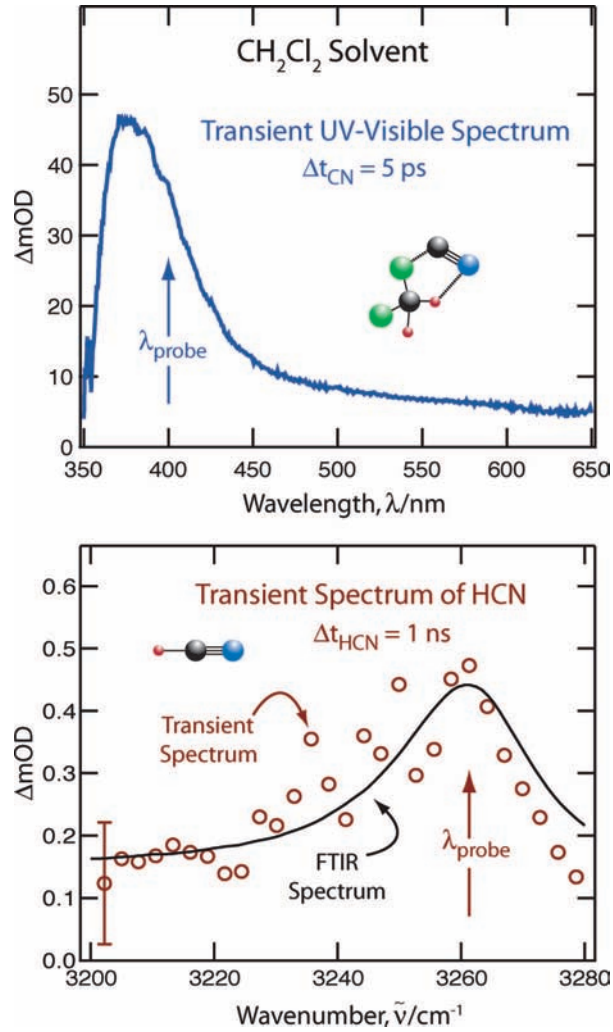

Figure 2. *Top Panel*: The UV−vis transient spectrum of CN radical in CH_2Cl_2 at a delay of $\Delta t_{CN} = 5$ ps. The structure in the panel is that of the bridging complex to which we primarily attribute this spectrum. The arrow for λ_{probe} marks the wavelength we use for monitoring the time evolution. *Bottom Panel*: The transient spectrum of HCN in CH_2Cl_2 at $\Delta t_{HCN} = 1$ ns. The open circles are the transient spectrum obtained from the infrared photodiode array, and the solid line is a conventional infrared spectrum obtained after a one-hour irradiation of the sample. The arrow for λ_{probe} marks the point we use for monitoring the time evolution, and the error bar shows the typical uncertainty for the measurements.

all of the solvents we study. In addition, a density functional theory calculation and molecular dynamics simulation finds the CN B ← X transition to be centered at 344 nm in water.[36] The top panel in Figure 2 is the transient UV−vis absorption spectrum that we obtain by introducing the broadband continuum probe at a delay of $\Delta t_{CN} = 5$ ps after the photolysis pulse in the solvent CH_2Cl_2. Its prominent maximum near 380 nm is likely the B ← X electronic transition that occurs at 388 nm for isolated CN radicals,[4] although the sharp decrease of the continuum probe intensity at shorter wavelengths prevents our locating the maximum precisely. The spectra for all of the other solvents have maxima at essentially the same location. We rule out the transition to a charge-transfer state of a CN−solvent complex because it should appear at a much longer wavelength than the transition we observe. The 550-nm transition of the CN−H_2O complex[29] would occur at even longer wavelengths in our more easily ionized solvents. Adjusting the transition energy for the water complex for the ionization energy

of our solvents predicts that the charge-transfer transitions lie beyond 1.2 μm.

It is also unlikely that the transition we observe arises from the I atom produced in the photolysis. The transient electronic absorption decays within a few nanoseconds, a time that is too short for the endothermic reaction of I with the solvent and too long for complexation dynamics. In addition, a rough estimate of the location of the charge-transfer transition for I, obtained by adjusting the $\lambda = 340$ nm transition for the $Cl-CH_2Cl_2$ complex[33] for the electron affinity of I and the ionization energy of the solvents,[13] predicts that all of these charge-transfer transitions are below 364 nm. Another potential origin of the absorption we observe is excitation of a charge-transfer transition in a complex of the solvent with an electronically excited I atom. A similar estimate of the transition energy in which we increase the electron affinity by the spin−orbit splitting of iodine predicts transitions for the I*−solvent complex in the range of 360 to 480 nm for our solvents. However, Moskun et al. showed that the I* channel is likely to be energetically inaccessible for 267 nm photolysis of ICN in water, and they did not observe the I^*-H_2O complex in photodetachment studies of I^- in water.[37] Because we also observe no transitions at wavelengths greater than 400 nm in any solvent, it is unlikely that I*−solvent complexes contribute significantly to our signals.

Using a fixed wavelength 400 nm probe (marked with a vertical arrow in Figure 2) to monitor the time evolution gives the best signal-to-noise ratio, and the top panel of Figure 3 shows the resulting transient absorption. The 1 ps coherent response of the neat solvent determines the time resolution of the measurement. The signal rises to a maximum in about 1 ps[38] and has two, well-separated decays of about 4 and 1500 ps. We identify the initial, rapid decay as both cage and diffusive geminate recombination, and we assign the subsequent, slow decay to reaction of CN with the solvent. In the first few picoseconds after photodissociation, solvent reorganization can cause the features to shift, but we observe no spectral changes during that time.

The complementary observation to the time evolution of the reactive CN radical is the appearance of the HCN reaction product, which we detect by transient infrared absorption in the region of the fundamental C−H stretching transition. The open points in the bottom panel of Figure 2 are the transient absorption spectrum of HCN formed in CH_2Cl_2 at a delay of $\Delta t_{HCN} = 1$ ns, and the solid line is the conventional infrared spectrum obtained after irradiating a 3 mL sample of 0.2 M ICN in CH_2Cl_2 with 55 μJ pulses of 267 nm light for one hour. The bottom panel in Figure 3 shows the transient infrared signal at the maximum in the absorption at 3261 cm^{-1} (marked with a vertical arrow in Figure 2) following photolysis of ICN in CH_2Cl_2. In all seven solvents we study, there is an early multiphoton signal that we remove by subtracting the background signal at the edge of the array (~3200 cm^{-1}) from the maximum. The data shown in Figure 3 for CH_2Cl_2 have the poorest signal-to-noise ratio of all the solvents we study.

Comparison of the decay of the CN radical absorption with the growth of the HCN product absorption in Figure 3 shows that their timescales differ by about a factor of 7, indicating that the two experiments are not probing simple loss of a reactant and formation of the corresponding product. Every solvent we studied shows this disparity with differences ranging from about a factor of 2.5 for 1-chlorobutane to a factor of 12 for 1,2-dichloroethane. This situation contrasts drastically with the behavior we have observed previously for the reaction of chlorine radicals with pentane in some of the same solvents,

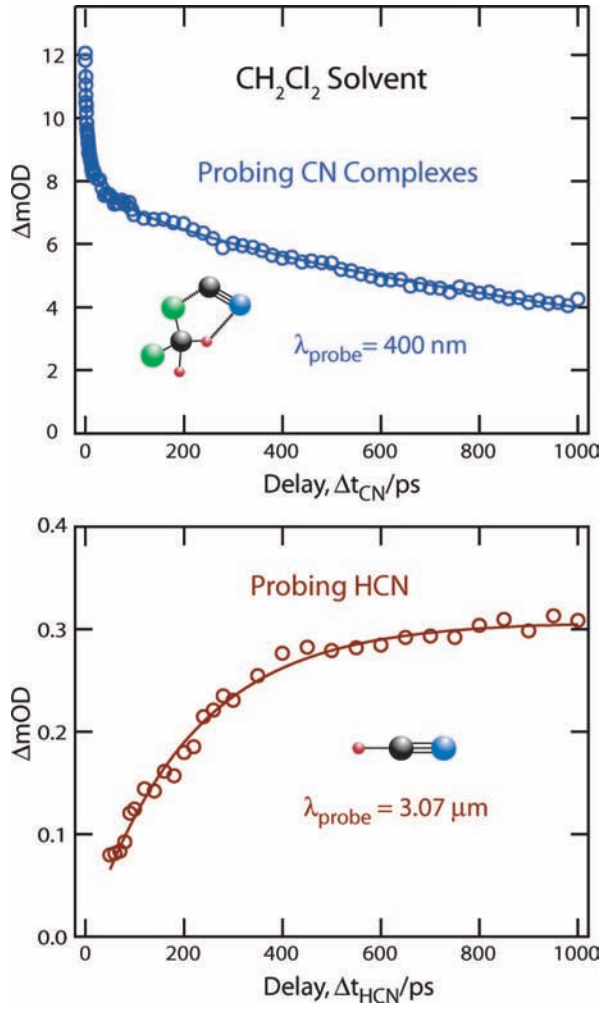

Figure 3. *Top Panel*: The time evolution of the $\lambda_{probe} = 400$ nm signal in CH_2Cl_2 following photolysis of ICN. *Bottom Panel*: The time evolution of the $\lambda_{probe} = 3.07$ μm (3261 cm^{-1}) signal in CH_2Cl_2 following photolysis of ICN. The solid lines in the figures are the fits of the kinetic model to the data using the parameters in Table 1.

where the decay times of the chlorine electronic absorption and the rise of the HCl vibrational transition are commensurate.[32] The slow loss of the reactants compared to the appearance of the products suggests that the two probes are observing species that are kinetically decoupled from each other. One possibility is that CN radicals rapidly complex with the solvent to form two species that react at different rates but have similar electronic spectra. As described below, a kinetic scheme that incorporates that possibility describes the measurements quantitatively, and we have performed electronic structure calculations on isolated complexes as a rudimentary test of the plausibility this picture.

B. Electronic Structure Calculations. We use the *Gaussian 03* suite of programs to perform electronic structure calculations of isolated CN−solvent complexes.[39] Including the effects of the bulk solvent, which may stabilize isolated complexes differently, would change our quantitative results but not the qualitative picture, as shown by test calculations where we include a continuum solvent. Density functional theory calculations on the $CN + CH_2Cl_2$ system at the B3LYP level of theory with the 6−31+G* basis set find the two geometry minima shown in Figure 4. There is a linear complex with the nitrogen of the CN radical positioned next to a hydrogen atom of CH_2Cl_2, and there is a bridging complex with the CN radical spanning an H atom and a Cl atom of CH_2Cl_2 with the carbon atom of

TABLE 1: Fitting Parameters

Solvent	Fixed Parameters		Adjustable Parameters			
	ϕ	A/ns$^{-1/2}$	k_{br}/ ns^{-1}	k_{lin}/ ns^{-1}	f_{lin}^{CN}	f_{lin}^{HCN}
1-chlorobutane	0.82	0.0055	4.05 ± 0.84	10.5 ± 1.3	0.21 ± 0.21	1.00 ± 0.16
2-chlorobutane	0.81	0.0045	3.52 ± 0.34	11.9 ± 1.8	0.03 ± 0.10	0.94 ± 0.15
2-chloropropane	0.79	0.0063	2.17 ± 0.21	16.1 ± 4.3	0.05 ± 0.07	0.83 ± 0.15
1,4-dichlorobutane	0.80	0.0045	2.72 ± 0.33	11.4 ± 2.0	0.03 ± 0.10	1.00 ± 0.18
1,2-dichloroethane	0.87	0.0035	1.00 ± 0.07	12.4 ± 2.2	0.00 ± 0.04	0.72 ± 0.11
dichloromethane	0.82	0.0065	0.67 ± 0.14	4.8 ± 1.4	0.03 ± 0.10	1.00 ± 0.50
chloroform	0.84	0.0083	0.45 ± 0.12	3.2 ± 1.9	0.00 ± 0.09	1.00 ± 0.50

the radical positioned near a Cl atom of the solvent. Including zero-point energies in the calculations gives stabilities of the complexes relative to separated CN and CH_2Cl_2 of 430 cm^{-1} for the linear complex and 1540 cm^{-1} for the bridging complex. There is a transition state between the two that lies 220 cm^{-1} below the energies of the separated reactants but far enough above the energies of the complexes that there is a barrier to interconversion. (Analysis using a kinetic scheme that includes interconversion of the two complexes also suggests that it is unimportant in this system.[40]) The minima that this simple density functional theory calculation predicts are certainly not quantitatively correct because of both the level of theory and the neglect of solvent interactions. Because our kinetic analysis finds that the two complexes interconvert slowly, it is likely that the complexes are more strongly bound than our calculations suggest.

The relative population at room temperature of the two states with these energies favors the lower energy bridging complex by a factor of 250 over the linear complex. Solvation can change these relative populations substantially, and the B ← X transition probability of the CN radical may be different in the two complexes. However, the greater stability of the bridging complex suggests that it is the more abundant species and, thus, responsible for most of the absorption at 400 nm. By contrast, the difference in the observed decay times, described below, and the calculated structure of the linear complex suggest that it is responsible for most of the products whose infrared absorption we observe. The weaker binding of the linear complex and the proximity of carbon of the CN radical to adjacent solvent molecules from which it can abstract a hydrogen atom make it more likely to form HCN than the bridging complex.

Heaven and co-workers have studied CN radical van der Waals complexes experimentally and theoretically.[24−27,41] They have observed a linear complex between H_2 and CN bound by 38 cm^{-1} with the H_2 located on the nitrogen of the CN radical,[24,27,41] and they have also detected a bent complex between Ar and CN bound by 102 cm^{-1} with an Ar−C−N angle of 140°,[25] qualitatively similar to the 132° Cl−C−N angle that we calculate for the bridging complex. There are also electronic structure calculations for the CN−H_2O complex that find a hydrogen bond-like linear conformation with a well depth of about 600 cm^{-1}.[36] These experiments and calculations are all consistent with the CN radical forming two complexes with characteristically different geometries. There are also gas-phase kinetics studies that suggest that complexes are important in CN radical reactions with saturated hydrocarbons. These experiments obtain negative activation energies of several hundred wavenumbers.[7,17−23] Because negative activation energies are often the kinetic signature of complex formation, it appears that even the relatively weak interactions between the radicals and hydrocarbons give complexation a role in CN radical chemistry.

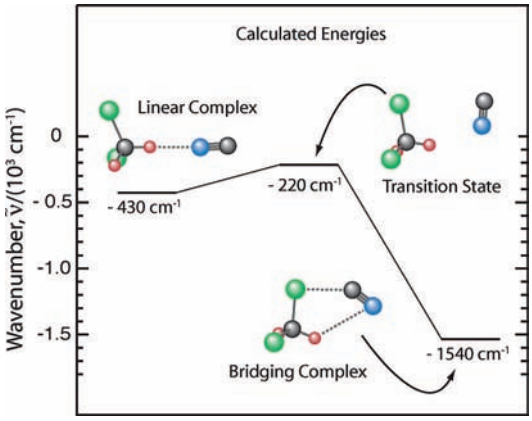

Figure 4. The calculated structures and energies of the CN−solvent complexes and the transition state for isomerization.

IV. Kinetic Analysis

Our observation of two different timescales for CN loss and HCN formation along with experiments and calculations implicating complexes in CN radical chemistry motivate our use of the kinetic scheme shown in Figure 5. In this scheme, rapid complexation forms two CN containing species that react at different rates following photolytic production of CN radicals. Figure 5 illustrates the kinetic scheme for the reaction with CH_2Cl_2, but we use it for all of the solvents we study. In this scheme, the complexation occurs in a few picoseconds and is much faster than any of the subsequent kinetics. Thus, the kinetics are essentially those of two independent species, the linear and bridging complexes, that react with rate constants k_{lin} and k_{br}, respectively. Both complexes contain the CN chromophore that we interrogate by transient absorption with $\lambda_{probe} = 400$ nm. They do not interconvert during the measurement, and both can potentially react to form the HCN product whose transient absorption we probe with $\lambda_{probe} = 3.07$ μm. The kinetic scheme shows the formation of HCN and ClCN explicitly, but our analysis only determines the total rate constant, k_{lin} or k_{br}, for the parallel reactions from each complex. Although the complexes could react to form other products, such as HNC, the formation of other products does not change the rate constants we extract. In fact, gas-phase studies of the reaction of CN radicals with hydrocarbons and $CHCl_3$ find negligible formation of HNC.[7,42]

These two rate constants and the fraction of the signal that comes from each complex are the important adjustable parameters for fitting the data. To fit data such as those shown in Figure 3 with this simple model, we also include a term in the transient absorption that accounts for the fast recombination of the initially formed CN radical. This term influences the fit to the rapid initial decay in the CN signal that is obvious in the data, but it does not influence the longer time behavior from

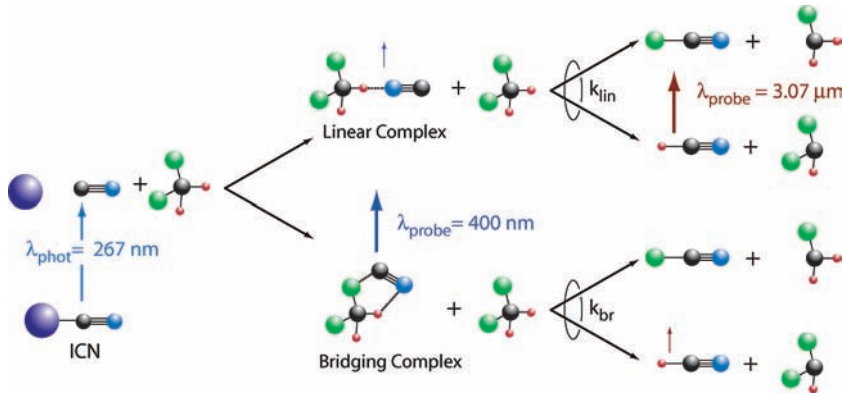

Figure 5. Kinetic scheme for photolysis of ICN, complex formation, and reaction of CN. Each complex reacts to form HCN or ClCN with different pseudo-first-order rate constants of k_{lin} for the linear complex (top) and k_{br} for the bridging complex (bottom). Fitting the transient absorption data shows that linear complex abstracts both H and Cl more rapidly than the bridging complex, which primarily abstracts Cl. The sizes of the vertical arrows for the probe transitions qualitatively indicate the relative contribution of each species to the transient absorption signal.

which we extract the rate constants and fractional contributions. The reactive loss of CN complexes and the formation of the HCN products follow the usual simple exponential decay and growth. Thus, we simultaneously fit the transient signals for CN, $S_{CN}(t)$, and for HCN, $S_{HCN}(t)$, to the expressions,

$$S_{CN}(t) = A_{CN}[1 - \phi erfc(A/\sqrt{t})][f_{lin}^{CN} e^{-k_{lin}t} + f_{br}^{CN} e^{-k_{br}t}] + A_{offset} \quad (1)$$

$$S_{HCN}(t) = A_{HCN}[f_{lin}^{HCN}(1 - e^{-k_{lin}t}) + f_{br}^{HCN}(1 - e^{-k_{br}t})] \quad (2)$$

The first term in brackets in eq 1 accounts for the removal of CN radicals by recombination using the Smoluchowski theory of diffusive recombination.[43,44] The parameter ϕ is the fractional recombination of the CN radical with its original partner radical I, and A comes from the rate of recombination. The second set of brackets in eq 1 contains the important terms that describe the bimolecular reaction of the complexes. In this expression, f_{lin}CN is the fraction of the CN transient absorption arising from the linear complexes, and f_{br}CN $= 1 - f_{lin}$CN is the fraction from the bridging complexes. The coefficient A_{CN} is an arbitrary amplitude, and A_{offset} accounts for a slowly decaying background signal that is essentially constant during the measurement.

The terms for the HCN transient absorption signal are analogous. The rate constants are the same in the two equations, and the fractional contributions of the linear and bridging complexes to the production of HCN are f_{lin}HCN and f_{br}HCN $= 1 - f_{lin}$HCN. Again, the coefficient A_{HCN} is an arbitrary amplitude, and there is no contribution of the recombination to the HCN signal during the times we analyze. Thus, the four essential fitting parameters are the two global rate constants, k_{lin} and k_{br}, and the fractional contribution of the linear complexes to the signal for CN and for HCN, f_{lin}CN and f_{lin}HC*N*.

The reaction rate constant data are insensitive to the details of recombination, and we are able to fix the ϕ and A terms. We use the $\phi = 0.84$ from a molecular dynamics simulation of $CHCl_3$[30] and scale it according to the viscosity of the solvent for the other systems we study.[45] Similarly, we take advantage of the insensitivity of the fits to the exact value of the parameter A to hold it constant at a value from an initial fit for each solvent. The offsets are $A_{offset} = 0.9$ mOD and $A_{offset} = 0.5$ mOD for the slowly reacting CH_2Cl_2 and $CHCl_3$ solvents respectively as determined in measurements with a 9 ns delay. The offset term is zero for all other solvents. We fit the HCN signal beginning with points at a delay of $\Delta t_{HCN} = 50$ ps to prevent imperfections in subtracting the multiphoton solvent response from affecting the results.

The solid lines in Figure 3 show the quality of fits that this model produces, and Table 1 collects the fitting parameters and associated uncertainties. The uncertainties are the amounts by which it is possible to change the parameters without an observable change in the quality of the fit. The recombination decay is essentially complete in 10 ps for all solvents, in agreement with previous measurements and molecular dynamics simulations of ICN photodissociation in $CHCl_3$.[28−30] The crucial results in the table are the rate constants and fractional contributions of the different complexes to the CN signal and the HCN signal, which we fit simultaneously. The fits yield a rate constant for the bridging complex, k_{br}, that is between a factor of 2.5 and 12 smaller than that for the linear complex, k_{lin}, depending on the solvent. This result is consistent with the more stable bridging complex giving up CN more slowly than the linear complex. The difference in the fractional contributions of the linear complexes to the CN signal and the HCN signal is particularly striking. The very small fractional contribution of linear complex to the evolution of the CN signal, f_{lin}CN ≈ 0, suggests that the more stable bridging complex dominates, f_{br}CN $= 1 - f_{lin}$CN ≈ 1, and determines the transient electronic absorption signal we observe. This behavior is again consistent with the more stable bridging complex being the most abundant species. By contrast, the linear complex is primarily responsible for the HCN time evolution, f_{lin}HCN ≈ 1, consistent with the more weakly bound complex reacting more readily and having a favorable geometry for hydrogen atom abstraction from the surrounding solvent.

IV. Discussion

Our observation of different times for the disappearance of the CN reactant absorption and the appearance of the HCN product absorption motivates our kinetic model incorporating two different CN complexes. Using this model to analyze the time evolution of the CN reactant and HCN product allows us to extract the reaction rate constants for CN complexes with seven different solvents. The rate constants for the complexes differ by as much as a factor of 10 among the solvents, a variation that appears to arise from a competition between differences in the number of labile atoms and differences in the transition states.

A. Complexes and Reaction Rates. The two previous studies of the decay of the CN transient absorption in $CHCl_3$ following photolysis of ICN[28,29] both fit the decay to a rapid component lasting a few picoseconds and a slower component lasting about 70 ps. Wan et al.[28] fit their data to a double

exponential form with time constants of $\tau_1 = (2.5 \pm 0.4)$ ps and $\tau_2 = (76 \pm 10)$ ps, and Moskun and Bradforth[29] use a similar scheme to obtain $\tau_1 = 4.0$ ps and $\tau_2 = 72$ ps. In the latter case, they also include a long time, constant signal and find that the three components have amplitudes of $A_1 = 31\%$, $A_2 = 27\%$, and $A_\infty = 42\%$. These fitting parameters reproduce our data rather well over the first 200 ps but do not agree at the longer times where we observe a continuing decay rather than the constant asymptote of their fit. Their experiments also observe a rapid rise of about 600 fs that is consistent with the rise we observe. Thus, all three measurements observe very similar decays over the time range that they have in common and find that the initial rapid decay comes from recombination of I and CN. However, our analysis of the longer time component shows that the decay does not simply reflect reaction to form HCN but involves the fate of the different complexes described above. Both of these previous studies focused on the short-time behavior and, in the case of Moskun and Bradforth, on the rotational dynamics of the initially formed CN radical. By contrast, we concentrate on the longer time behavior and possible reaction pathways.

The first time-resolved study of the reaction of CN radicals following photolysis of ICN in $CHCl_3$ used transient infrared absorption to monitor the production of HCN and ClCN. It showed that HCN appeared with an exponential time constant of $\tau_{HCN} = (194 \pm 20)$ ps and that ClCN appeared with a time constant of $\tau_{ClCN} = (140 \pm 36)$ ps.[2] By comparison, a similar fit to our data in Figure 3 yields a time constant of $\tau_{HCN} = (313 \pm 93)$ ps. The time constant corresponding to our more elaborate model, $k_{lin}^{-1} = (312 \pm 185)$ ps, is the same with a larger uncertainty owing to the more complicated model. The appearance time of ClCN measured in those experiments is also consistent with reaction of the linear complex, which forms both HCN and ClCN in our kinetic scheme. The slower reaction of the bridging complex should also produce a slower rise over a period of a few nanoseconds that may be present in the data but is difficult to discern over the 1 ns observation window.[2] Although our analysis consistently obtains a slightly longer reaction time to produce HCN, the results agree satisfactorily in light of our uncertainties. The most important point is that the model illustrated in Figure 5, which involves two complexes reacting a different rates, reproduces both the slow decay of the transient electronic absorption and the rapid growth of the transient vibrational absorption.

The key to our analysis is linking the absorptions to two different complexes. Fitting the data for all seven solvents using the kinetic scheme with two complexes (Figure 5) yields the results in Table 1. The fractional contributions of each of the complexes to the signal show that one complex, which we assign as the bridging complex, is responsible for the transient electronic absorption, and that another complex, which we assign as the linear complex, is responsible for production of the HCN that we observe by transient vibrational absorption. Calculations of the energies of the isolated complexes find that the bridging complex is more stable and, thus, likely less reactive than the linear complex. The relative reactivity of the complexes is not built into the model but is an inference from the fits. The negligible contribution of the bridging complex to the production of HCN implies that it primarily reacts to form other products (or decays by a nonreactive pathway). The calculated structure of the bridging complex, in which the CN spans a chlorine atom and a hydrogen atom with the carbon of the CN adjacent to chlorine, suggests that a likely reaction path is abstraction of chlorine within the complex and subsequent separation of the ClCN + CH_2Cl products. Thus, we expect that the bridging complex primarily reacts to form ClCN because formation of HCN within the complex is unlikely and the CN radical is poorly positioned to abstract a hydrogen atom from the surrounding solvent. By contrast, the relatively weakly bound linear complex, in which the CN is bound to hydrogen through its nitrogen atom, is ideally positioned to react with surrounding solvent molecules by abstracting either a hydrogen atom to form HCN or a chlorine atom to form ClCN. In this picture, the linear complex forms both products, and the rate constant k_{lin} reflects those two parallel processes, whose relative probability we do not know. Perhaps coincidentally, the activation energy of 420 cm^{-1} that Raftery et al.[2] obtain from the temperature dependence of the production of HCN from the reaction of CN with $CHCl_3$ is close to the binding energy we calculate for the linear complex.

Our analysis finds that the two complexes have different reaction rates, product pathways, and stabilities. We can use the transient absorption of HCN that we measure in CH_2Cl_2 to make a rough estimate of the relative concentration of the complexes. Using the infrared extinction coefficient of $\epsilon_{HCN} = 326$ $cm^{-1}M^{-1}$ for HCN,[2] a path length of 1 mm, and our measured HCN absorption of 0.31 mOD, we calculate a concentration of 10 μM for HCN. Using the approximation that the amount of ClCN produced by the linear complex is comparable to the amount of HCN, we estimate an initial concentration of linear complexes of about 20 μM. Using our measured extinction coefficient for ICN at 267 nm, $\epsilon_{CN} = 86$ $cm^{-1}M^{-1}$, and our beam conditions, we calculate that the initial concentration of CN that escapes the solvent cage after photolysis is 520 μM.[46] Assuming that all of those CN radicals form one of the two complexes, we estimate that the concentration of bridging complexes is 500 μM, a 25 fold excess over the concentration of linear complexes. Thus, both our calculation of the relative energies of the isolated complexes and our experimental estimate of the relative amounts show that the bridging complex is the dominant species in solution. Our picture of the reaction is that the CN radicals rapidly form two different complexes with the solvent. Most of the complexes have a relatively stable bridging structure and react relatively slowly to form primarily ClCN but a few of them have a less stable linear structure and react relatively rapidly to form, in part, the HCN products that we observe.

B. Correlation of Solvent Structure and Reactivity. Our measurements and analysis for seven different solvents provide the pseudo-first-order reaction rate constants for the reaction of CN complexes with those solvents. They have different extents of chlorine substitution and range from methane derivatives (chloroform and dichloromethane) to butane derivatives (chlorobutane and dichlorobutane). This range of sizes and substitutions allows us to search for correlations of the structure of the solvent with its reactivity. Studies of hydrogen abstraction by chlorine radicals have established a correlation between chlorine atom substitution and a change in the rate of abstraction of α and β hydrogens.[47−49] These correlations are the basis of quantitative structure activity relationships that predict the reaction rate constant from the number and positions of the chlorine substitutents.[48,50] The structure activity relationships empirically predict the rate of hydrogen abstraction by chlorine from any chlorinated alkane by assigning a rate constant to each primary, secondary, and tertiary hydrogen based on its position. Weighting each contribution by a factor that depends on the neighboring substituents and summing all of the contributions gives the predicted rate constant. Sheps et al. have shown that these relationships correctly predict the *relative* rates for the

TABLE 2: Second-Order Rate Constants and Fractional Cl Content

solvent	f_{Cl}	$C_{solvent}$/M	$k^2_{br}/10^9$ M^{-1}s^{-1}	$k^2_{lin}/10^9$ M^{-1}s^{-1}
1-chlorobutane	0.10	9.6	0.42 ± 0.09	1.1 ± 0.1
2-chlorobutane	0.10	9.4	0.37 ± 0.04	1.3 ± 0.2
2-chloropropane	0.13	11	0.20 ± 0.02	1.5 ± 0.4
1,4-dichlorobutane	0.20	9.1	0.30 ± 0.04	1.3 ± 0.2
1,2-dichloroethane	0.33	12.7	0.079 ± 0.006	1.0 ± 0.2
dichloromethane	0.50	15.6	0.043 ± 0.009	0.31 ± 0.09
chloroform	0.75	12.4	0.036 ± 0.010	0.26 ± 0.15

reactions of chlorinated alkanes in solution.[33] They also found that the abstraction rate decreased with increased chlorine content in a series of chlorinated butanes, in accord with the structure activity relationships and consistent with chlorine substitution changing the stability of the transition state to increase the activation energy.

Our measurements of the reactivity of the CN complexes show some of the same qualitative trends as chlorine atom abstraction of hydrogen atoms in gases and liquids. To compare the rates for the different solvents, we divide the pseudo-first-order rate constants for the two complexes in Table 1, k_{lin} and k_{br}, by the concentration of the neat solvent to obtain the corresponding second-order rate constants, k^2_{lin} and k^2_{br}. Table 2 lists these rate constants along with the fraction of the labile atoms that are chlorine, f_{Cl}, for each solvent. Figure 6, which gives the second-order rate constants for the solvents in order of increasing chlorine content, shows that the reaction rate constants for both the linear and bridging complexes decrease as the fraction of the labile atoms that are chlorine increases. The second-order rate constant for the linear complex, k^2_{lin}, is roughly the same for all the butanes and perhaps slightly larger for 2-chloropropane, but it decreases noticeably for 1,2-dichloroethane, dichloromethane, and chloroform. These three, which have Cl fractions ranging from $f_{Cl} = 0.33$ to 0.75, are clearly less reactive than the other four, which have fractions between 0.10 and 0.20. The second-order rate constant for the bridging complex, k^2_{br}, follows a similar pattern with the rate constant falling sharply for 1,2-dichloroethane. There is a general correlation of slower reaction with greater Cl content, but it is likely that this trend does not solely reflect the replacement of labile hydrogen atoms by less reactive chlorine atoms. The variation in the rate constants that we found previously for chlorine atom reactions[31] reflects changes in the transition state for hydrogen abstraction,[33,47−49] and those same effects seem important in the analogous reactions of CN radicals.

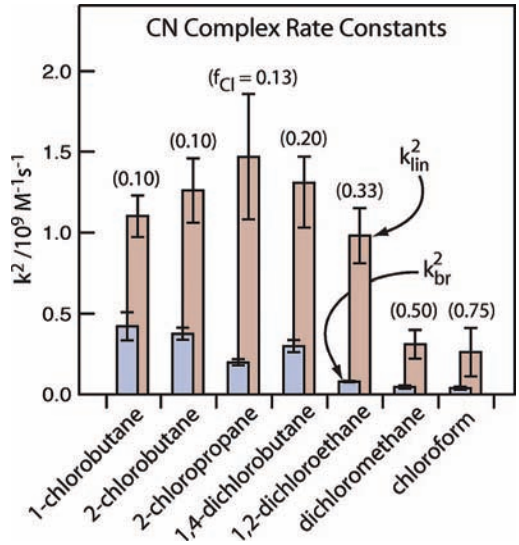

Figure 6. The second-order bimolecular rate constants for bridging and linear complexes, k^2_{br} and k^2_{lin}. The solvents are listed in order of increasing chlorine content, and f_{Cl} is the fraction of labile atoms in each solvent that are chlorine.

V. Summary

Time-resolved studies of the reaction of CN radicals with a series of chlorinated alkanes using transient absorption to observe the evolution of the reactants and of the products indicate that CN radicals rapidly form two different types of complexes with the solvent. One of the complexes is linear with CN bound to a hydrogen atom of the solvent through its nitrogen atom, and the other complex is bent with the CN bridging a chlorine atom and a hydrogen atom of the solvent with its carbon atom connected to the chlorine. The experiments probe the CN radical by its electronic absorption near 400 nm and interrogate the HCN product by the infrared absorption of the C−H stretch near 3.07 μm. The observation that the CN signal disappears more slowly than the HCN signal appears suggests that the two species are decoupled from each other kinetically, as would be the case if the CN radical rapidly formed complexes with the solvent. Electronic structure calculations on isolated complexes of CN with CH_2Cl_2 find that there are two complexes with different stabilities. The relatively weakly bound linear complex is likely to abstract either hydrogen or chlorine atoms readily from the solvent to form HCN ClCN, and the more strongly bound bridging complex is likely to react more slowly to produce primarily ClCN. Fitting the transient signals, we observe to this kinetic model shows that the linear complex reacts up to 12 times faster than the bridging complex. The analysis also shows that the bridging complex is responsible for the slow decay of the CN transient absorption and that the linear complex is responsible for the rapid formation of the HCN product. The details of the structure of the reacting solvent molecules influence the reaction rates of both complexes. Increasing the fractional Cl content of the solvent slows the reaction rate for both complexes, reflecting both the different reactivities of the H and Cl atoms and the changes that chlorine substitution makes in the transition state for the reaction.

Acknowledgment. We thank the National Science Foundation for supporting this work, and A.C.C. gratefully acknowledges an NSF predoctoral fellowship. We thank Professor Frank Weinhold for many useful discussions concerning electronic structure calculations, and we are grateful to Professor Martin Zanni for the use of his infrared photodiode array.

References and Notes

(1) Elles, C. G.; Crim, F. F. *Annu. Rev. Phys. Chem.* **2006**, *57*, 273.
(2) Raftery, D.; Gooding, E.; Romanovsky, A.; Hochstrasser, R. M. *J. Chem. Phys.* **1994**, *101*, 8572.
(3) Raftery, D.; Iannone, M.; Phillips, C. M.; Hochstrasser, R. M. *Chem. Phys. Lett.* **1993**, *201*, 513.
(4) Herzberg, G. *Molecular Spectra and Molecular Structure I. Spectra of Diatomic Molecules*, 2nd ed.; Van Nostrand Reinhold Company: New York, 1950.
(5) *CRC Handbook of Chemistry and Physics*; 77 ed.; Lide, D. R., Ed.; CRC Press Inc.: Boca Raton, 1996.
(6) Morris, V. R.; Mohammad, F.; Valdry, L.; Jackson, W. M. *Chem. Phys. Lett.* **1994**, *220*, 448.
(7) Copeland, L. R.; Mohammad, F.; Zahedi, M.; Volman, D. H.; Jackson, W. M. *J. Chem. Phys.* **1992**, *96*, 5817.
(8) Samant, V.; Hershberger, J. F. *Chem. Phys. Lett.* **2008**, *460*, 64.
(9) Huang, C.; Li, W.; Estillore, A. D.; Suits, A. G. *J. Chem. Phys.* **2008**, *129*, 074301.
(10) Alfassi, Z. B.; Huie, R. E.; Mittal, J. P.; Neta, P.; Shoute, L. C. T. *J. Phys. Chem.* **1993**, *97*, 9120.

(11) Shoute, L. C. T.; Neta, P. *J. Phys. Chem.* **1990**, *94*, 2447.
(12) Shoute, L. C. T.; Neta, P. *J. Phys. Chem.* **1990**, *94*, 7181.
(13) Chateauneuf, J. E. *Chem. Phys. Lett.* **1989**, *164*, 577.
(14) Chateauneuf, J. E. *J. Am. Chem. Soc.* **1990**, *112*, 442.
(15) Chateauneuf, J. E. *J. Org. Chem.* **1999**, *64*, 1054.
(16) Elles, C. G.; Cox, M. J.; Barnes, G. L.; Crim, F. F. *J. Phys. Chem. A* **2004**, *108*, 10973.
(17) Lichtin, D. A.; Lin, M. C. *Chem. Phys.* **1986**, *104*, 325.
(18) Atakan, B.; Wolfrum, J. *Chem. Phys. Lett.* **1991**, *186*, 547.
(19) Yang, D. L.; Yu, T.; Wang, N. S.; Lin, M. C. *Chem. Phys.* **1992**, *160*, 307.
(20) Georgievskii, Y.; Klippenstein, S. J. *J. Phys. Chem. A* **2007**, *111*, 3802.
(21) Herbert, L.; Smith, I. W. M.; Spencer-Smith, R. D. *Int. J. Chem. Kinet* **1992**, *24*, 791.
(22) Balla, J. R.; Casleton, K. H.; Adams, J. S.; Pasternack, L. *J. Phys. Chem.* **1991**, *95*, 8694.
(23) Sims, I. R.; Queffelec, J.-L.; Travers, D.; Rowe, B. R.; Herbert, L.; Karthaeser, J.; Smith, I. W. M. *Chem. Phys. Lett.* **1993**, *211*, 461.
(24) Heaven, M. C.; Buchachenko, A. A. *J. Mol. Spectrosc.* **2003**, *222*, 31.
(25) Han, J. D.; Heaven, M. C.; Schnupf, U.; Alexander, M. H. *J. Chem. Phys.* **2008**, *128*, 104308.
(26) Chen, Y. L.; Heaven, M. C. *J. Chem. Phys.* **2000**, *112*, 7416.
(27) Kaledin, A. L.; Heaven, M. C.; Bowman, J. M. *J. Chem. Phys.* **1999**, *110*, 10380.
(28) Wan, C. Z.; Gupta, M.; Zewail, A. H. *Chem. Phys. Lett.* **1996**, *256*, 279.
(29) Moskun, A. C.; Bradforth, S. E. *J. Chem. Phys.* **2003**, *119*, 4500.
(30) Benjamin, I. *J. Chem. Phys.* **1995**, *103*, 2459.
(31) Moskun, A. C.; Jailaubekov, A. E.; Bradforth, S. E.; Tao, G. H.; Stratt, R. M. *Science* **2006**, *311*, 1907.
(32) Sheps, L.; Crowther, A. C.; Carrier, S. L.; Crim, F. F. *J. Phys. Chem. A* **2006**, *110*, 3087.
(33) Sheps, L.; Crowther, A. C.; Elles, C. G.; Crim, F. F. *J. Phys. Chem. A* **2005**, *109*, 4296.
(34) Larsen, J.; Madsen, D.; Poulsen, J. A.; Poulsen, T. D.; Keiding, S. R.; Thogersen, J. *J. Chem. Phys.* **2002**, *116*, 7997.
(35) We stir 14 g (0.29 mol) of NaCN in 200 mL of cold distilled H_2O until dissolved and add 62 g (0.24 mol) of I_2 in four approximately equal steps. After stirring for 90 minutes, we add 200 mL of cold ether and stir for 10 minutes. We separate the H_2O layer into two equal parts and extract each part three times with 90 mL of cold ether. We evaporate the ether and recrystallize the dry yellowish-white product in 1.8 L cyclohexane and wash the product with cyclohexane to remove residual water and I_2. After 4 hours of air drying, the product typical yield is typically 10−12 g (27−32%) of white, fluffy crystals.
(36) Pieniazek, P. A.; Bradforth, S. E.; Krylov, A. I. *J. Phys. Chem. A* **2006**, *110*, 4854.
(37) Moskun, A. C.; Bradforth, S. E.; Thogersen, J.; Keiding, S. *J. Phys. Chem. A* **2006**, *110*, 10947.
(38) In the neat solvent, there is a coherence feature that unambiguously determines the zero of time. In ICN solutions, we cannot use this feature and instead fit the signal rise to the convolution of an instantaneous rise with a Gaussian pulse. Comparing the neat solvent and the ICN solution shows that the center of the best-fit Gaussian pulse occurs 0.34 ps after the coherence feature, which establishes the zero of time for all of the measurements.
(39) Frisch, M. J. T., G. W.; Schlegel, H. B.; Scuseria, G. E.; Robb, M. A.; Cheeseman, J. R.; Montgomery,Jr., J. A.; Vreven, T.; Kudin, K. N.; Burant, J. C.; Millam, J. M.; Iyengar, S. S.; Tomasi, J.; Barone, V.; Mennucci, B.; Cossi, M.; Scalmani, G.; Rega, N.; Petersson, G. A.; Nakatsuji, H.; Hada, M.; Ehara, M.; Toyota, K.; Fukuda, R.; Hasegawa, J.; Ishida, M.; Nakajima, T.; Honda, Y.; Kitao, O.; Nakai, H.; Klene, M.; Li, X.; Knox, J. E.; Hratchian, H. P.; Cross, J. B.; Bakken, V.; Adamo, C.; Jaramillo, J.; Gomperts, R.; Stratmann, R. E.; Yazyev, O.; Austin, A. J.; Cammi, R.; Pomelli, C.; Ochterski, J. W.; Ayala, P. Y.; Morokuma, K.; Voth, G. A.; Salvador, P.; Dannenberg, J. J.; Zakrzewski, V. G.; Dapprich, S.; Daniels, A. D.; Strain, M. C.; Farkas, O.; Malick, D. K.; Rabuck, A. D.; Raghavachari, K.; Foresman, J. B.; Ortiz, J. V.; Cui, Q.; Baboul, A. G.; Clifford, S.; Cioslowski, J.; Stefanov, B. B.; Liu, G.; Liashenko, A.; Piskorz, P.; Komaromi, I.; Martin, R. L.; Fox, D. J.; Keith, T.; Al-Laham, M. A.; Peng, C. Y.; Nanayakkara, A.; Challacombe, M.; Gill, P. M. W.; Johnson, B.; Chen, W.; Wong, M. W.; Gonzalez, C.; and Pople, J. A. *Gaussian 03*, Rev. B.05; Gaussian, Inc.: Wallingford CT, 2004.
(40) This scheme uses two complexes, A and B. Complex A can isomerize into complex B, which reacts with the solvent to form HCN or ClCN. Thus, both complexes contribute to the electronic absorption, but all of the production of HCN comes from complex B. The best fit of the data using this scheme produces an isomerization rate constant of zero.
(41) Chen, Y. L.; Heaven, M. C. *J. Chem. Phys.* **1998**, *109*, 5171.
(42) Arunan, E.; Manke, G.; Setser, D. W. *Chem. Phys. Lett.* **1993**, *207*, 81.
(43) Tachiya, M. *Radiat. Phys. Chem.* **1983**, *21*, 167.
(44) Rice, S. A. *Diffusion-Limited Reactions*; Elsevier Science Publishing Company Inc.: New York, 1985.
(45) The Smoluchowski expressions and the inverse proportionality between the diffusion constant and the viscosity allow us to write the recombination fraction $\phi = (1-C\eta^{-1/2})$ where η is the viscosity of the solvent. Using the value $\phi = 0.84$ from the molecular dynamics simulation of CN in $CHCl_3$, we calculate C and use it along with the viscosity of each of the other solvents to estimate ϕ for that solvent.
(46) The calculation of the CN radical concentration from photolysis uses a beam diameter of 80 μm, a pulse energy of 8 μJ, a path length of 1 mm, and an ICN concentration of 0.2 M along with a cage escape fraction of 15%.
(47) Kelly, C. C.; Wijnen, M. H. J. *J. Phys. Chem.* **1969**, *73*, 2447.
(48) Senkan, S. M.; Quam, D. *J. Phys. Chem.* **1992**, *96*, 10837.
(49) Dobis, O.; Benson, S. W. *J. Phys. Chem. A* **2000**, *104*, 5503.
(50) Aschmann, S. M.; Atkinson, R. *Int. J. Chem. Kinet.* **1995**, *27*, 613.

JP8064079